PHYSICAL REVIEW LETTERS

Electron-Vibration Interaction in Single-Molecule Junctions: From Contact to Tunneling Regimes

O. Tal,[1] M. Krieger,[1,2] B. Leerink,[1] and J. M. van Ruitenbeek[1]

[1]*Kamerlingh Onnes Laboratory, Leiden University, P.O. Box 9504, 2300 RA Leiden, The Netherlands*
[2]*Institute of Applied Physics, University of Erlangen-Nürnberg, Staudtstrasse 7/A3, D-91058 Erlangen, Germany*

Point contact spectroscopy on a H_2O molecule bridging Pt electrodes reveals a clear crossover between enhancement and reduction of the conductance due to electron-vibration interaction. As single-channel models predict such a crossover at a transmission probability of $\tau = 0.5$, we used shot noise measurements to analyze the transmission and observed at least two channels across the junction where the dominant channel has a $\tau = 0.51 \pm 0.01$ transmission probability at the crossover conductance, which is consistent with the predictions for single-channel models.

PACS numbers: 73.63.Rt, 72.10.Di, 73.40.−c, 73.63.Nm

A molecule bridging between two metallic electrodes provides the opportunity to explore the interactions between mechanical motion (molecular vibrations) and electron transport at the atomic scale. The influence of a vibration mode on the conductance of such junctions is measured by inelastic electron tunneling spectroscopy (IETS) [1,2] or by point contact spectroscopy (PCS) [3,4]. Both spectroscopies were originally developed for macroscopic junctions. IETS was first investigated for molecules buried inside a metal-oxide-metal tunneling junction [5] and was later applied to single-molecule junctions using scanning tunneling microscopy (STM) [1]. PCS was first investigated for the study of electron-phonon interactions in metal wires with a submicron size constriction [6], and it was latter applied to single atom [3] and molecule junctions [4] formed by mechanically controlled break junctions (MCBJs). These techniques provide information on the presence of the molecule [7,8], its structure [4], the molecule orientation [9], and the molecule-leads coupling [10]. Essentially, IETS and PCS are associated with a similar measurement of current (or its first and second derivatives) as a function of voltage between the two leads but operate in the opposite limits of low conductance ($G \ll 1G_0$, where $G_0 = 2e^2/h$ is the conductance quantum) for IETS [1] and conductance close to $1G_0$ for PCS [4], respectively.

In off-resonance [11] IETS and PCS measurements, above a certain voltage bias, the incoming electrons have sufficient energy to scatter inelastically by exciting a vibration mode at the junction. Interestingly, electron-vibration interaction leads to an increase in the junction conductance for junctions in the tunneling regime (e.g., IETS done by STM [1]); however, it decreases the conductance for junctions in the contact regime (e.g., PCS across a Pt/H_2 junction [4]). The conductance enhancement in the first case is commonly explained by the opening of an additional tunneling channel for electrons that lost energy to a vibration mode [5]. The conductance

suppression in the second case has been explained in the limit of perfect electron transmission probability ($\tau = 1$) by backscattering of electrons that lose energy to a vibration mode and are then restricted by Fermi statistics to taking on the opposite momentum, since at $\tau = 1$ the forward momentum states are fully occupied at the reduced energy [12].

For weak electron-vibration interaction, the effect of vibration excitation on the conductance is determined merely by the transmission probability across the junction, when using models based on the lowest order expansion [13] of the electron-vibration coupling [14–16] and for symmetric coupling of the molecule to both leads [17,18]. In this framework, which is different from the simplified view presented above, a combined picture for the two limits (tunneling and contact) was suggested by several single-level models [14,16–18]. The models predict conductance enhancement below a transmission probability of $\tau = 0.5$ and suppression of conductance above this, due to two opposite contributions to the conductance by the electron-vibration interaction: an inelastic scattering process that increases the conductance and an elastic process, where a virtual phonon is emitted and reabsorbed by the electron. The latter effect reduces the conductance [15]. In spite of the theoretical efforts invested in exploring the different regimes of the electron-vibration interactions in atomic and molecular junctions, this issue has not been addressed experimentally.

In this Letter, we present PCS and shot noise measurements across a single-molecule break junction formed by Pt electrodes and H_2O molecules. By altering the electrode distance, we have measured the effect of the electron-vibration interaction on the differential conductance (dI/dV) in the transition between tunneling and contact regimes [19]. The main transmission channels across the junctions and their probabilities were determined by allowing comparison with single-channel models that ascribe changes in the electron-vibration interaction to the value of
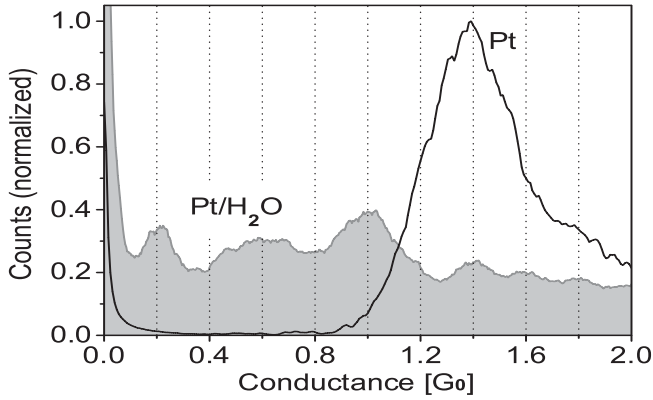
FIG. 1. Conductance histograms (normalized to the area under the curves and set to 1 at the Pt peak) for a Pt junction (black curve) and for Pt after introducing H_2O (solid curve). Each conductance histogram is constructed from 1000 conductance traces recorded with a bias of 0.2 V during repeated breaking of the contact.

the transmission probability. Our findings provide experimental support for these models and expand their implications to junctions involving multiple channels.

The Pt/H_2O molecular junctions were formed by using an MCBJ setup [3] at about 5 K. Clean Pt electrode apexes are formed under cryogenic vacuum conditions by breaking a notched Pt wire (polycrystalline, 0.1 mm diameter, 99.99% purity). The wire was broken by mechanical bending of a flexible substrate to which the wire was attached. The interelectrode distance can be accurately adjusted (with subatomic precision) by fine bending of the substrate using a piezoelement. The formation of a clean Pt contact is verified by conductance histograms made from 1000 conductance traces taken during repeated contact stretching as presented in Fig. 1 (black curve). The single peak around $1.4G_0$ provides a fingerprint of a clean Pt contact [4].

Deionized H_2O [20] was placed in a quartz tube and was degassed by four cycles of freezing, pumping, and thawing. While the Pt junction was broken and formed repeatedly, H_2O molecules were introduced to the junction through a heated capillary (baked out prior to cooling). The junction exposure to H_2O is controlled by a leak valve at the top of the capillary and by the capillary temperature. Following water introduction, the typical Pt peak in the conductance histogram is suppressed, and contributions from a wide conductance range are detected (see Fig. 1, solid curve) with minor peaks around 0.2, 0.6, and $1.0G_0$ (peaks around 0.95 and $1.10G_0$ are sometimes observed as well). The continuum in the conductance counts implies a variety of stable junction configurations that we exploit for spectroscopy measurement on junctions with different conductance as discussed next.

Figure 2 presents differential conductance measurements as a function of voltage across the Pt/H_2O junction at two different zero-voltage conductance values: (a) $1.02 \pm 0.01G_0$ and (b) $0.23 \pm 0.01G_0$. Junctions with
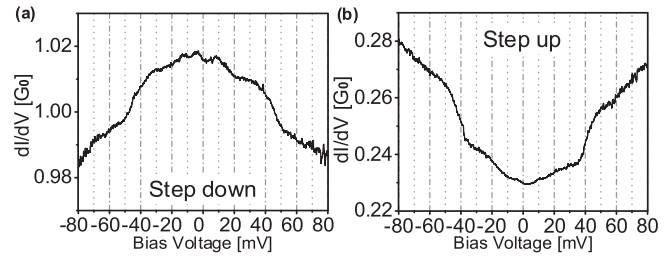

FIG. 2. Differential conductance (dI/dV) as a function of the bias voltage for two different Pt-H_2O-Pt junctions with zero-bias conductance of (a) $1.02 \pm 0.01G_0$ and (b) $0.23 \pm 0.01G_0$. Above a certain bias voltage, the energy of the incoming electrons exceeds the energy of a molecular vibration mode, and some of the electrons (a few percent) lose energy by exciting the vibration mode. Consequently, the conductance drops [steps down, (a)] or is enhanced [steps up, (b)] by the electron-vibration scattering.

different zero-bias conductance are formed by altering the distance between the Pt contacts or by readjusting a new contact. The steps in the conductance that appear at 46 mV in Fig. 2(a) and 42 mV in Fig. 2(b) indicate the onset of a vibration excitation at these voltages (the origin of the steps as due to the electron-vibration interaction was verified by isotope substitution; see, e.g., [1,9]). Vibration modes around 42 meV are typical for Pt/H_2O junctions and may be associated with a rotation mode [21]. While in (a) the differential conductance is decreased ("step down"), curve (b) taken at lower zero-voltage conductance shows an increase in the differential conductance ("step up"). These two examples demonstrate that both conductance suppression and enhancement can be observed at a relatively high conductance (much higher than the typical tunneling conductance).

Collecting many dI/dV spectra at different zero-voltage conductance values allows us to focus on the transition between the two cases. Figure 3 presents the distribution of
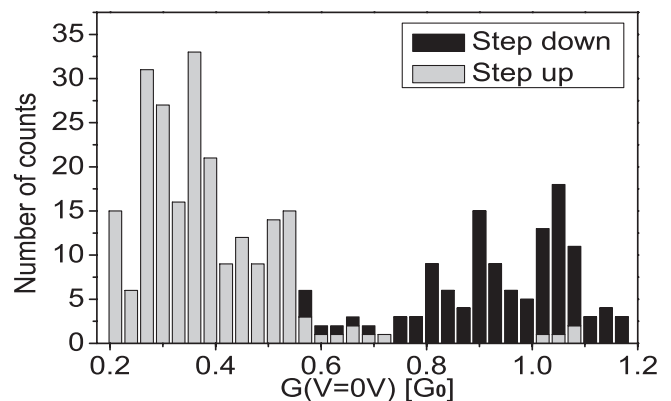

FIG. 3. Histogram of step-up (gray) and step-down (dark) features in dI/dV spectra for a Pt/H_2O junction as a function of zero-bias conductance. A crossover is observed between 0.57 and $0.72 \pm 0.03G_0$.

differential conductance curves with step up (gray) and step down (dark) according to their zero-voltage conductance. Curves with step up appear below $0.57 \pm 0.03G_0$, and curves with step down were detected only above $0.72 \pm 0.03G_0$. Thus, the crossover between conductance enhancement to conductance reduction by the electron-vibration interaction occurs between these two values.

According to the single-channel models, the crossover is expected at a transmission probability of $\tau = 0.5$ ($\tau < 0.5$) for junctions with similar (different) coupling to the electrodes and in any case not higher than $\tau = 0.5$ [17,18]. The measured conductance at the crossover is above $0.5G_0$. However, more than one channel can contribute to the measured conductance as demonstrated by Landauer's formula [22,23]: $G = G_0\sum_i \tau_i$, where τ_i is the transmission probability of the ith channel across the junction. In order to examine our findings in view of the theoretical predictions, we determined the number of transmission channels and their probability by using shot noise measurements.

Shot noise results from time-dependent fluctuations in the electrical current caused by the discreteness of the electron charge. When electrons flow across a point contact (e.g., a single atom or molecule junction), the noise level is determined by the number of available transmission channels across the junction and their transmission probabilities τ_i. The total noise level of a quantum point contact for temperature T and applied bias voltage V is given by [24]:

$$S_I = 2eV \coth\left(\frac{eV}{2kT}\right)\frac{2e^2}{h}\sum_i \tau_i(1-\tau_i) + 4kT\frac{2e^2}{h}\sum_i \tau_i^2,$$

(1)

where k is Boltzmann's constant. Thus, in combination with Landauer's equation, the main transmission probabilities can be resolved from noise and conductance measurements.

We have measured noise by using the method described in Ref. [25]. Once a stable contact was established at a certain conductance, the noise power was measured as a function of frequency at different current bias values, where at each bias 10 000 noise spectra were averaged. dI/dV spectra were measured before and after every set of noise measurements to verify that the same contact was maintained during the measurements and to avoid junctions with considerable dI/dV fluctuation within the measurement bias range (conductance fluctuations are ascribed to electron interference due to scattering centers in the vicinity of the junction [26]). The noise at nonzero bias is composed from thermal and shot noise [see Eq. (1); both are white noise in the measured frequency range of 0–100 KHz] and $1/f$ noise [27]. Since the noise signal is suppressed at high frequencies due to the low-pass characteristic of the measurement setup, the data were corrected for the transfer characteristics obtained from the thermal noise which was measured at zero bias [25]. The $1/f$ noise contribution was identified by its dependence on
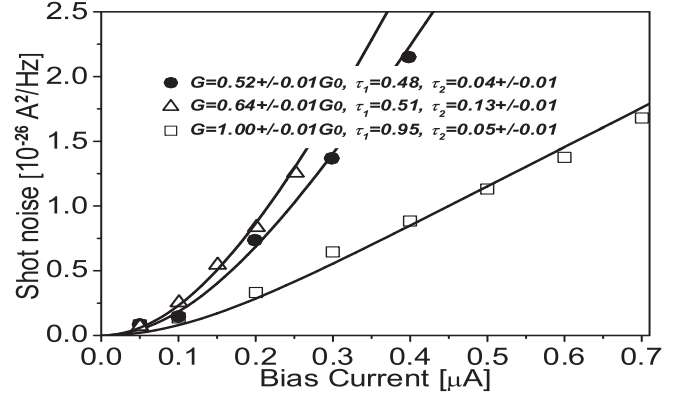

FIG. 4. Shot noise as a function of the bias current. The symbols present shot noise measured on contacts with $G = 0.52 \pm 0.01G_0$ (bullets), $G = 0.64 \pm 0.01G_0$ (open triangles), and $G = 1.00 \pm 0.01G_0$ (open squares). Fitting the data with Eq. (1) (solid curves) gives the decomposition of the total conductance in terms of the conduction channels (τ_1 and τ_2).

V^2 (unlike the shot noise dependence on V) and was removed from the curves taken at nonzero bias. Finally, the thermal noise is removed by subtraction of the curve taken at zero bias from the rest of the curves taken at different finite biases.

Following this, analysis several sets of shot noise as a function of current bias were obtained for junctions with different zero-bias conductance. Figure 4 presents three examples for such data taken on junctions with zero-bias conductance of 0.52 (bullets), 0.64 (open triangles), and $1.00 \pm 0.01G_0$ (open squares) zero-bias conductance. The transmission probability of the main channels can be determined by fitting Eq. (1) to the measured noise and using Landauer's equation to obtain the total transmission probabilities from the measured conductance. Since the fitting is extremely sensitive to the number of channels and their probabilities [25,28], the freedom in choosing the main transmission probability is limited, in this case to ± 0.01, while choosing more than two channels is restricted to small additional channels that do not affect the main probability (in the range of ± 0.01).

The main transmission probabilities obtained for junctions with different conductance are presented in Table I. The reliability of the noise measurements is demonstrated by the consistency of the transmission probabilities be-

TABLE I. Zero-bias conductance, total transmission probability (τ), main transmission probabilities (τ_1 and τ_2), and the ratio between the main transmission probability and the total transmission for different Pt/H$_2$O junctions.

$G[G_o]$, τ	0.52	0.62	0.64	0.96	1.00	± 0.01
τ_1	0.48	0.51	0.51	0.93	0.95	± 0.01
τ_2	0.04	0.11	0.13	0.03	0.05	± 0.01
τ_1/τ [%]	92 ± 2	82 ± 2	80 ± 2	97 ± 1	95 ± 1	

tween independent measurements done on different junctions with relatively close conductance (e.g., 0.62 and $0.64 \pm 0.01 G_0$ or 0.96 and $1.00 \pm 0.01 G_0$). Keeping in mind the prediction for inversion in the electron-vibration effect at a single transmission probability of 0.5, it is interesting to examine the main transmission probability at different conductance values. At $0.52 G_0$ the main transmission probability is lower than 0.5, whereas at $0.96 G_0$ it is well above 0.5. The main transmission probability crosses 0.51 ± 0.01 at a conductance of 0.62–$0.64 G_0$.

By considering both PCS and shot noise measurements, we observe a clear crossover between enhancement of the differential conductance to suppression at 0.57–$0.72 G_0$. It is found that all of the examined junctions have one transmission channel which is dominant over the other channel(s) (fourth row of Table I). Finally, the transmission probability of the dominant channel crosses $\tau = 0.51 \pm 0.01$ at a zero-bias conductance of 0.62–$0.64 G_0$, right at the center of the conductance range where the crossover between differential conductance enhancement to suppression takes place. The agreement of these findings with the single-channel models that predict a transition at $\tau = 0.5$ provided that the molecule coupling to both electrodes is similar suggests that the latter condition is fulfilled and that the conductance suppression or enhancement by the electron-vibration interaction is determined by the value of the *dominant* transmission probability. From a more general perspective, the lowest order expansion for the electron-vibration interaction correctly predicts a crossover in sign of the step in differential conductance at transmission of $\tau = 0.5$. Even in the presence of additional conductance channels, this effect can be observed for the dominant channel, as in the case for our Pt/H_2O system.

When there is not a single dominant channel [as was observed for Pt/C_6H_6 (benzene) junctions [29]], no clear transition between conductance enhancement to suppression is observed. However, many other junctions follow the general behavior of step down near $1 G_0$ (e.g., Au atomic wires [3] and Pt/H_2 [4]) and step up below $0.3 G_0$ (e.g., Ag atomic wires decorated with oxygen [30]).

[1] B. C. Stipe, M. A. Rezaei, and W. Ho, Science **280**, 1732 (1998).
[2] H. Park, J. Park, A. K. L. Lim, E. H. Anderson, A. P. Alivisatos, and P. L. McEuen, Nature (London) **407**, 57 (2000).
[3] N. Agraït, C. Untiedt, G. Rubio-Bollinger, and S. Vieira, Phys. Rev. Lett. **88**, 216803 (2002).
[4] R. H. M. Smit, Y. Noat, C. Untiedt, N. D. Lang, M. C. van Hemert, and J. M. van Ruitenbeek, Nature (London) **419**, 906 (2002).
[5] R. C. Jaklevic and J. Lambe, Phys. Rev. Lett. **17**, 1139 (1966).
[6] I. K. Yanson, Zh. Eksp. Teor. Fiz. **66**, 1035 (1974) [Sov. Phys. JETP **39**, 506 (1974)].
[7] X. H. Qiu, G. V. Nazin, and W. Ho, Phys. Rev. Lett. **92**, 206102 (2004).
[8] L. H. Yu, Z. K. Keane, J. W. Ciszek, L. Cheng, M. P. Stewart, J. M. Tour, and D. Natelson, Phys. Rev. Lett. **93**, 266802 (2004).
[9] D. Djukic, K. S. Thygesen, C. Untiedt, R. H. M. Smit, K. W. Jacobsen, and J. M. van Ruitenbeek, Phys. Rev. B **71**, 161402(R) (2005).
[10] E. A. Osorio, K. O'Neill, M. Wegewijs, N. Stuhr-Hansen, J. Paaske, T. Bjørnholm, and H. S. J. van der Zant, Nano Lett. **7**, 3336 (2007).
[11] A. Troisi and M. A. Ratner, Small **2**, 172 (2006).
[12] N. Agraït, C. Untiedt, G. Rubio-Bollinger, and S. Vieira, Chem. Phys. **281**, 231 (2002).
[13] M. Galperin, M. A. Ratner, and A. Nitzan, J. Chem. Phys. **121**, 11 965 (2004).
[14] M. Paulsson, T. Frederiksen, and M. Brandbyge, Phys. Rev. B **72**, 201101(R) (2005).
[15] J. K. Viljas, J. C. Cuevas, F. Pauly, and M. Häfner, Phys. Rev. B **72**, 245415 (2005).
[16] L. de la Vega, A. Martín-Rodero, N. Agraït, and A. Levy Yeyati, Phys. Rev. B **73**, 075428 (2006).
[17] M. Paulsson, T. Frederiksen, H. Ueba, N. Lorente, and M. Brandbyge, arXiv:0711.3392v1 [Phys. Rev. Lett. (to be published)].
[18] R. Egger and A. O. Gogolin, Phys. Rev. B **77**, 113405 (2008).
[19] T. Frederiksen, N. Lorente, M. Paulsson, and M. Brandbyge, Phys. Rev. B **75**, 235441 (2007).
[20] Milli-Q water: $R > 18.2$ MΩ cm at 25 °C.
[21] This mode is insensitive to contact stretching and to variations in the junction conductance. More definite identification requires detailed comparison with calculations.
[22] R. Landauer, IBM J. Res. Dev. **1**, 223 (1957).
[23] R. Landauer, Philos. Mag. **21**, 863 (1970).
[24] Y. M. Blanter and M. Büttiker, Phys. Rep. **336**, 1 (2000).
[25] D. Djukic and J. M. van Ruitenbeek, Nano Lett. **6**, 789 (2006).
[26] B. Ludoph and J. M. van Ruitenbeek, Phys. Rev. B **61**, 2273 (2000).
[27] P. Dutta and P. M. Horn, Rev. Mod. Phys. **53**, 497 (1981).
[28] H. E. van den Brom and J. M. van Ruitenbeek, Phys. Rev. Lett. **82**, 1526 (1999).
[29] M. Kiguchi, O. Tal, S. Wohlthat, F. Pauli, M. Krieger, D. Djukic, J. C. Cuevas, and J. M. van Ruitenbeek, arXiv:0803.0563v1.
[30] W. H. A. Thijssen, M. Strange, J. M. J. aan de Brugh, and J. M. van Ruitenbeek, New J. Phys. **10**, 033005 (2008).